FISEVIER

Contents lists available at ScienceDirect

Materials Science & Engineering C

journal homepage: www.elsevier.com/locate/msec



Visible light-assisted efficient degradation of dye pollutants with biomass-supported ${\rm TiO_2}$ hybrids



Hun Xue^a, Yilan Chen^{a,c}, Xinping Liu^a, Qingrong Qian^a, Yongjin Luo^a, Malin Cui^b, Yisong Chen^b, Da-Peng Yang^{b,*}, Qinghua Chen^{a,*}

- a College of Environmental Science and Engineering, Fujian Normal University, Fujian Key Laboratory of Pollution Control & Resource Reuse, Fuzhou, China
- ^b College of Chemical Engineering and Materials Science, Quanzhou Normal University, Quanzhou, China
- ^c College of Ecological Environment and Urban Construction, Fujian University of Technology, Fuzhou, China

ARTICLE INFO

Keywords: Photocatalyst Methyl orange Sugarcane bagasse Titanium oxide

ABSTRACT

The objective of this work was to develop a novel organic-inorganic hybrid nanomaterial from agricultural biomass waste for environmental applications. The sugarcane bagasse (SB) supported $\rm TiO_2$ hybrids were firstly synthesized via a sol-gel method. A series of characterizations were carried out to reveal the structures and components of obtained hybrids. Due to organic-inorganic hybrid (OIH) effect and element doping, the SB-TiO₂ hybrid can expand its optical absorbance ranging from ultraviolet to visible light. The optimal hybrid catalyst prepared with SB doping amount of 2 g in 100 mL titanic gel and calcined at 200 °C was able to degradate 95.0% methyl orange (MO) in 5 h under visible light. This study will pave a new and facile pathway for novel visible light driven photocatalysts based on $\rm TiO_2$ modified by agricultural biomass waste.

1. Introduction

Semiconductor photocatalysis has been considered as one of facile, low-cost, clean and environmentally friendly techniques in air purification, wastewater treatment, heavy metal remediation, sterilization, etc. [1-5]. Among various semiconductor materials, titanium oxide (TiO₂) is the most commonly used photocatalyst for its economy, nontoxicity, reusability, efficient catalytic activity. However, TiO2 can only absorb ultraviolet light which accounts for < 5% of the sunlight's energy for its wide band gap (3.2 eV) [6,7]. To obtain visible light responsive TiO₂-based photocatalysts, various modified methods have been studied, including surface deposition of noble metals [8], coupling with other semiconductors [9,10], surface photosensitization [11,12], doping with various metal and nonmetal elements [13-16], with organic materials [17-20], etc. Organic-inorganic hybrid (OIH) materials used for catalysts, delivery, therapy, sensors, and so on have attracted much attention [21–26]. OIH materials decorating ${\rm TiO_2}$ typically shows improved mechanical, optical, and thermal properties than pure TiO2. When TiO₂ hybridized with organic materials, its light absorbance range can be expanded. It has been reported that TiO2-based OIH materials (e.g. $TiO_2/microcrystalline$ cellulose, TiO_2/β -cyclodextrin and TiO₂/polyvinyl alcohol, etc.) show high catalytic activity for organic pollutant degradation under visible irradiation [17–19].

Agricultural biomass wastes are inexpensive and readily available

natural organic resources [27–29]. Sugarcane bagasse (SB), composing of cellulose (40–45%), hemicellulose (30–35%) and lignin (20–30%), is one of the most abundant agro-industrial residues. The annual output of dry bagasse is about 234 million tons throughout the world and most bagasse is burnt to produce energy for mills. However, a considerable amount is still left as waste and causes serious environmental problems [30–32]. To the best of our knowledge, OIH photocatalytic material based on TiO_2 modified by agro-industrial residues is seldom reported.

In spite of granular TiO_2 nanoparticles possess excellent photocatalytic activity, their recovery and reuse are difficult when they are used in aqueous, resulting in the waste and secondary pollution [33–36]. To improve the reusability of TiO_2 , TiO_2 was decorated by SB. Moreover, SB with large surface area and high porosity can be used as an adsorbent for the purification of wastewater containing dyes and heavy metals [37,38]. Therefore, SB- TiO_2 hybrid material will contact completely with pollutants and contribute to the improvement of photocatalytic activity of SB- TiO_2 .

In this study, an OIH material TiO_2 -SB was synthesized by sol-gel method and used as photocatalyst for the degradation of azo dye methyl orange (MO) under visible light irradiation. Synthetic conditions were optimized to achieve the highest photocatalytic activity. This hybrid photocatalyst represents a new type of efficient and inexpensive photocatalytic material with high visible light utilization.

E-mail addresses: yangdp@qztc.edu.cn (D.-P. Yang), cqhuar@fjnu.edu.cn (Q. Chen).

^{*} Corresponding authors.

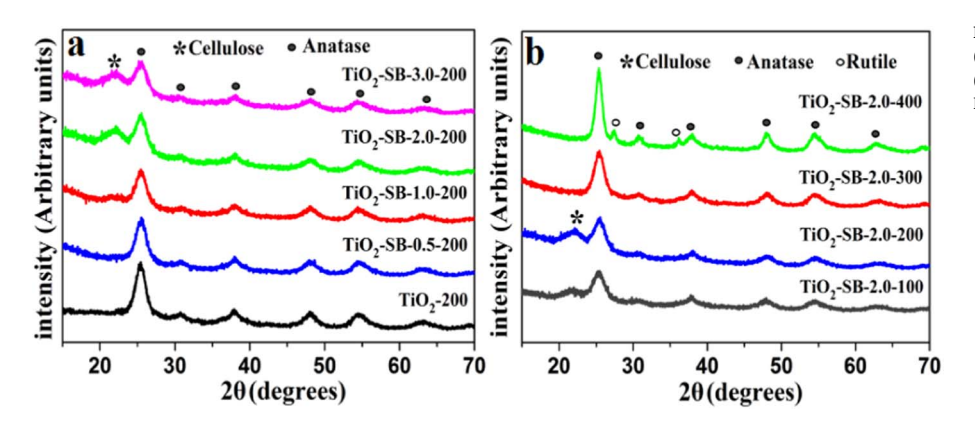


Fig. 1. XRD patterns of (a) TiO₂-200 and TiO₂-SB-m-200 (m = 0.5 g, 1.0 g, 2.0 g, and 3.0 g). (b) TiO₂-SB-2.0-T (T = 100 °C, 200 °C, 300 °C, and 400 °C). (♠) Anatase. (○) Rutile. (*) Cellulose.

2. Experimental

2.1. Synthetic procedure

TiO₂-SB was prepared by a sol-gel method. Typically, titanium tetraisopropoxide was hydrolyzed under acidic conditions and the resulting suspension was dialyzed to pH of $\sim\!4$. Then a transparent TiO₂ sol formed [39] and was calcined to prepare TiO₂ powder under 200 °C for 5 h. This TiO₂ power is denoted as TiO₂-200. On the other hand, a set mass (0.5 g, 1.0 g, 2.0 g, or 3.0 g) of SB was added to 100 mL TiO₂ sol and stirred for 2 h at room temperature. These gels were placed in a muffle furnace and heated at 5 °C/min to fixed temperature (100 °C, 200 °C, 300 °C, or 400 °C) and maintained for 5 h. Finally, samples TiO₂-SB-m-T were obtained, where m stands for the starting SB masses and T is the calcination temperatures.

2.2. Characterization

Phase identification of TiO_2 -200, TiO_2 -SB-m-T (m = 0.5 g, 1.0 g, 2.0 g, and 3.0 g) and TiO2-SB-2.0-T were conducted with X-ray diffraction (XRD) (Bruker D8) with CuKa radiation. The accelerating voltage and the applied current were 40 kV and 40 mA, respectively. The crystallite size was calculated from X-ray line broadening analysis by Scherrer equation: $D = 0.89\lambda / \beta \cos\theta$, where D is the crystal size in nm, λ is the CuKa wavelength (0.15406 nm), β is the half-width of the peak in rad, and θ is the corresponding diffraction angle. Thermogravimetric analyse (TGA) was performed on a Netzsch Sta 449C thermal analysis instrument. Measurement was taken with a heating rate of 5 °C/min from 30 to 800 °C. Morphology of the sample was characterized by field emission scanning electron microscopy (FESEM) (JSM-6700F). Transmission electron microscopy (TEM) and high resolution transmission electron microscopy (HRTEM) images were taken by JEOL model JEM 2010 EX instrument at an accelerating voltage of 200 kV. The powder particles were supported on a carbon film coated on a 3 mm diameter fine-mesh copper grid. A suspension in ethanol was sonicated and dripped on the carbon film supported by 300-mesh Cu grids. Nitrogen-sorption isotherms were analyzed at 77 K using a BELSORP-mini II equipment. All samples were degassed at 100 °C under vacuum for 3 h prior to measurement. FT-IR spectra were captured in transmittance mode with a resolution of 4 cm⁻¹ using a Nicolet Nexus 670 FT-IR spectrometer. UV-vis diffuse reflectance spectra (DRS) were measured by Varian Cary 500 with an integrating sphere using BaSO₄ as the reference. X-ray photoelectron spectra (XPS) were recorded on a PHI Quantum 2000 XPS System with a monochromatic Al Ka source and a charge neutralizer. All binding energies were referenced to the C1s peak at 284.8 eV of the surface adventitious carbon.

2.3. Photocatalytic activity measurements

The visible-light source was a 500 W halogen lamp (Philips Electronics) positioned beside a cylindrical reaction vessel with a plane side. The reaction system was maintained to be the room temperature by wind and running water. The 420 nm and 800 nm cut-off filters were placed before the vessel to eliminate the interference from visible-light wavelengths. Prepared photocatalysts (80 mg) were suspended in 80 mL of MO aqueous solution (3×10^{-5} mol/L) and stirred for 2 h before irradiation to ensure that the adsorption/desorption equilibrium had been reached. A 4 mL aliquot was taken at 1 h intervals during the experiment and centrifuged. The resulting clear liquor was analyzed on a Shimadzu UV–vis-NIR spectrophotometer (UV-1750). The percentage of degradation is reported as C/C_0 , where C is the absorbance of MO at 464 nm at each irradiated time interval, and C_0 is the absorbance of the MO solution at the initial adsorption/desorption equilibrium.

3. Results and discussion

3.1. X-ray diffraction analysis

The XRD patterns of the control TiO $_2$ -200 and samples TiO $_2$ -SB-m-200 are shown in Fig. 1a. Compared with typical diffraction peak of standard anatase TiO $_2$ (JCPDS No. 21-1272), TiO $_2$ were suggested to be anatase TiO $_2$. A diffraction peak at 22.5° is attributed to cellulose in SB [37]. This peak is absent in the TiO $_2$ -SB-0.5-200 sample possibly due to the low content of SB. With the increasing of SB content, the characteristic diffraction peak of anatase TiO $_2$ weakens and broadens, indicating that SB has a negative effect on the growth of TiO $_2$ crystals. The average crystal diameters of TiO $_2$ -200 and TiO $_2$ -SB-m-200 were calculated from Scherrer equation based on the half-width of the strongest diffraction peak of anatase TiO $_2$ and the results are 20 nm, 13 nm, 9 nm, 6 nm, and 5 nm for TiO $_2$ -200 and TiO $_2$ -SB-m-200 (m = 0.5, 1.0, 2.0, and 3.0 g), respectively.

As shown in Fig. 1b, the samples prepared below 300 °C are anatase ${\rm TiO_2}$ and the diffraction peak intensities were improved with the increasing of calcination temperature, suggesting higher calcination temperature play a key role on the crystallization of ${\rm TiO_2}$. ${\rm TiO_2}$ in ${\rm TiO_2}$ -SB-2.0-400 composed of anatase and rutile, suggesting the crystalline of ${\rm TiO_2}$ changes from anatase to rutile at high temperature. The diffraction peak of cellulose disappears when the calcination temperature was above 200 °C, this can be contributed to the decomposition of cellulose at a high temperature.

3.2. TGA measurement

Fig. 2 shows the TGA curves of SB and TiO_2 -SB-2.0. There are two stages on the SB curve from 30 °C to 800 °C. Between 30 and 100 °C, a weight loss of about 1.5% can be attributed to the loss of water molecules from SB. Dramatic weight loss of 98% between 220 and 500 °C

Download English Version:

https://daneshyari.com/en/article/5434178

Download Persian Version:

https://daneshyari.com/article/5434178

Daneshyari.com